Hepatic tumors: pitfalls in diagnostic imaging

Giulia Grazzini[1], Diletta Cozzi[1], Federica Flammia[1], Roberta Grassi[2], Andrea Agostini[3,4], Maria Paola Belfiore[2], Alessandra Borgheresi[4], Maria Antonietta Mazzei[5], Chiara Floridi[3,4], Gianpaolo Carrafiello[6], Andrea Giovagnoni[3,4], Silvia Pradella[1], Vittorio Miele[1]

[1] Department of Radiology, Careggi University Hospital, Florence, Italy; [2] Department of Precision Medicine, University of Campania "L. Vanvitelli", Naples, Italy; [3] Department of Clinical, Special and Dental Sciences, University Politecnica delle Marche, Ancona, Italy; [4] Division of Special and Pediatric Radiology, Department of Radiology, University Hospital "Umberto I - Lancisi - Salesi", Ancona, Italy; [5] Unit of Diagnostic Imaging, Department of Medical, Surgical and Neuro Sciences and of Radiological Sciences, University of Siena, Azienda Ospedaliero-Universitaria Senese, Siena, Italy; [6] Radiology Department, Fondazione IRCCS Cà Granda, Ospedale Maggiore Policlinico, Milan, Italy

Summary. On computed tomography (CT) and magnetic resonance imaging (MRI), hepatocellular tumors are characterized based on typical imaging findings. However, hepatocellular adenoma, focal nodular hyperplasia, and hepatocellular carcinoma can show uncommon appearances at CT and MRI, which may lead to diagnostic challenges. When assessing focal hepatic lesions, radiologists need to be aware of these atypical imaging findings to avoid misdiagnoses that can alter the management plan. The purpose of this review is to illustrate a variety of pitfalls and atypical features of hepatocellular tumors that can lead to misinterpretations providing specific clues to the correct diagnoses. (www.actabiomedica.it)

Keywords: CT, MRI, hepatocellular tumors, hepatocellular adenoma, focal nodular hyperplasia, hepatocellular carcinoma

Introduction

According to the classification of hepatocellular nodules by the International Working Party in 1995 and further elaboration by the International Consensus Group for Hepatocellular Neoplasia in 2009, hepatocellular nodules are divided into regenerative lesions including focal nodular hyperplasia (FNH), and dysplastic or neoplastic lesions, which comprise hepatocellular adenoma (HCA), dysplastic nodule (DN), and hepatocellular carcinoma (HCC) (1). Diagnostic imaging is a fundamental step for characterizing a wide range of pathologies (2-12), and in the abdominal field, we can take advantage of a multiparametric assessment through ultrasound, computed tomography (CT) and magnetic resonance imaging (MRI) (13-21). Typical imaging features of hepatocellular nodular lesions are well known (22). However, FNH, HCA, and HCC can show unu-

sual findings or share an overlap in radiological characteristics leading to diagnostic challenges. Differentiation of benign from malignant lesions is essential for an appropriate management plan (23-25).

In this review, we profile both typical and atypical imaging features of hepatocellular tumors on CT and MRI for being aware of radiologic pitfalls and for achieving the correct diagnosis.

Focal Nodular Hyperplasia

FNH is the most common benign hepatocellular lesion (up to 8% of all liver neoplasms), occurs primarily in women of reproductive age (80% of cases), and is often discovered incidentally (26-28). FNH is thought to arise from a vascular anomaly leading to a hyperplastic response with disorganized growth of hepatocytes and bile ducts. As the FNH management is usually

conservative, a definitive diagnosis should be obtained by imaging in order to avoid biopsy. However, atypical imaging FNH presentations can occur so that diagnosis could be a challenge. Typical FNHs are solitary, non-capsulated with a central fibrous scar (53% of FNHs overall), and are usually smaller than 5cm (27). On non-enhanced CT, FNH is usually iso- or hypodense to the adjacent liver parenchyma. Thanks to its multiparametric properties, MRI is highly sensitive and specific for the characterization of focal liver lesions (29). On unenhanced MRI, FNH is typically iso- or moderate hypointense on T1-weighted images and iso- or moderate hyperintense on T2-weighted images (30). The central scar appears as a thin band hypointense on T1 and hyperintense on T2-weighted images **(fig. 1)** (31). On contrast-enhanced CT and MRI, FNHs typically undergo immediate, intense, homogeneous enhancement on arterial phase and enhancement similar to the liver on portal venous and delayed phases **(fig. 1)** (30). The central scar is characterized by a delayed enhancement due to fibrotic content (32, 33).

In literature, the prevalence of atypical FNHs varies from 10% to 50%, and a wide range of atypical imaging findings have been described (26). On T1-weighted images, FNHs can appear hyperintense due to intralesional steatosis, hemorrhage, copper accumulation, or peliosis (26). In 10-37% of cases, FNHs show a pseudocapsule that results from compression of the adjacent hepatic parenchyma leading to differential diagnosis with HCC (26).

The primary differential diagnosis of the typical FNH includes HCA, which demonstrates a similar enhancement pattern. Usually, the diagnosis of FNH or HCA is possible thanks to characteristic lesion features such as the central scar in FNHs or the heterogeneous appearance due to intralesional hemorrhage in HCA (34). However, in up to 50% of cases, FNHs do not exhibit the central scar, especially in lesions smaller than 3cm, and, also, they can occasionally show heterogeneous signal on MRI (35). Therefore, hepatobiliary (HB) contrast-enhanced MRI is mandatory to differentiate FNHs from HCAs. MRI performed with HB contrast agent (the most common are Gd-BOPTA, MultiHance, Bracco, Milan, Italy and Gd-EOB-DTPA, Primovist; Bayer Schering Pharma, Germany) is considered the gold standard in imaging FNH (32, 34). Furlan A. et al., in their study on FNHs occurred after chemotherapy treatment, demonstrated that typical MRI
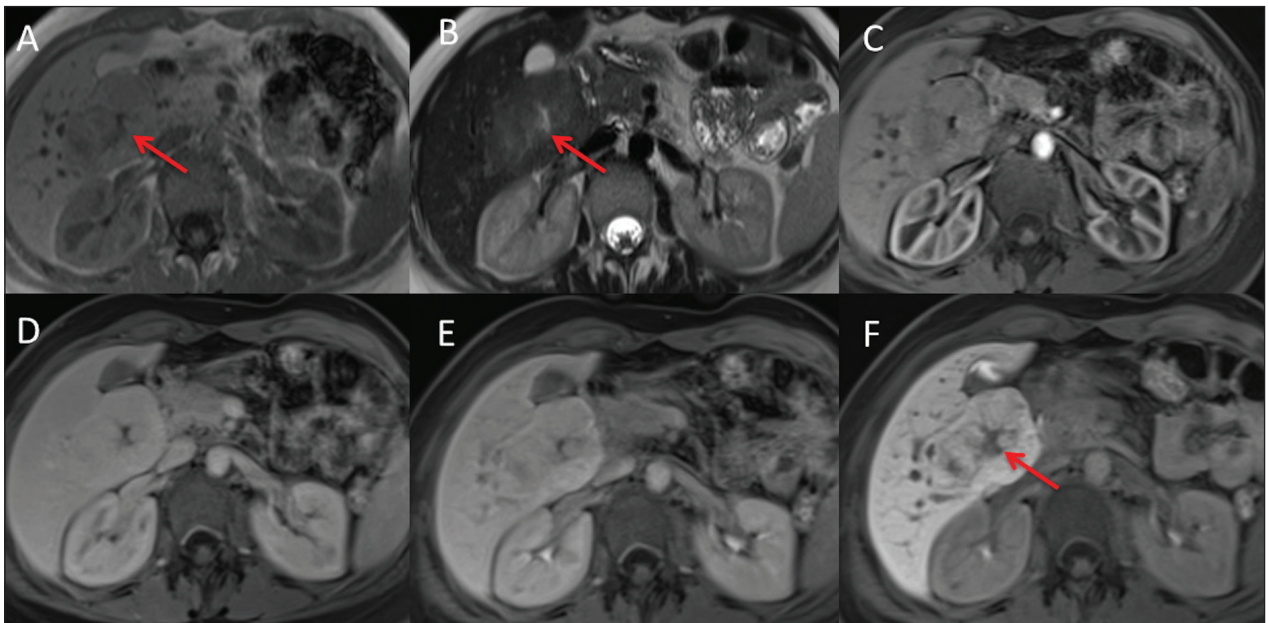

Figure 1. FNH with the central scar on Gd-EOB-DTPA-enhanced MRI. The typical FNH shows a central scar (arrows) that appears as a hypointense band on T1 (A) and hyperintense on T2-weighted images (B). On contrast-enhanced MRI, FNH undergoes immediate enhancement on arterial phase (C) and enhancement similar to the liver on portal venous and late, delayed phases (D-E). In the hepatocyte phase, FNH shows isointensity with the central scar hypointense (F)

appearance might avoid unnecessary biopsy or surgery (36). A particular finding of FNHs is iso- or hyperintensity in the hepatocyte phase with the central scar hypointense **(fig. 1)** (37, 38). On the contrary, in HCAs, the failure uptake of HB contrast agents on hepatocyte phase leads to hypointensity relative to a background enhanced normal liver parenchyma (34, 35).

The central fibrous scar is not specific for FNH, and other lesions, such as haemangiomas and fibrolamellar HCCs, may show it (32). Fibrolamellar HCC is a variant that usually occurs in young adults without chronic liver disease. The clues to the correct diagnosis of fibrolamellar HCCs are features such as hypointensity of the central scar on both T1- and T2-weighted images and hypointensity on the HB phase, different from FNHs (38).

In the cirrhotic liver, especially in patients with alcoholic cirrhosis or in liver showing hemodynamic changes, such as Budd Chiari syndrome, hyperplastic nodules called FNH- like nodules (FNH-LNs) has been reported. These hypervascular lesions may mimic tumors such as metastasis, HCA, or HCC. FNH-LN can show marked arterial enhancement or a wash-out and capsule appearance on CT or MRI, as HCC dose (39, 40). However, as FNH, FNH-LNs uptake HB contrast agents on hepatocyte phase showing iso- or hyperintensity (39).

Hepatocellular Adenoma

HCA is an uncommon benign tumor (annual incidence of 3-4/100000) that usually affects young females with a history of prolonged oral contraceptive use (41). Recent studies suggest obesity and metabolic syndrome as emerging risk factors for HCA, too (41). HCA is characterized by cords of well-differentiated hepatocytes separated by sinusoids lacking portal triad and interlobular bile ducts (27, 28).

The most common complication of HCA is bleeding with the risk of hemorrhagic rupture, while malignant degeneration occurs in a small subset of HCAs (around 4-5% of HCAs) (27).

According to 2010 WHO classification, four subtypes of HCA are described based on their genetic and pathologic features: inflammatory HCA (I-HCA), hepatocyte nuclear factor (HNF)-1α-inactivated

HCA, β-catenin-mutated HCA (β-HCA), and unclassified HCA (U-HCA) (28, 37). These subtypes show noticeable differences in imaging features. The latest 2017 Genotype/Phenotype Classification of HCAs categorized HCAs into eight major subtypes. The four additional subtypes were previously within the U-HCA category, and they have not yet been associated with specific diagnostic imaging features (41).

MRI plays a crucial role in the diagnosis and subtype characterization of HCAs, helping to differentiate HCAs from HCCs and FNHs (41, 42). Bise S. et al. analyzed MRI features of 116 HCAs reporting that MRI can identify up to 88% of the two main HCA subtypes (I-HCA and HNF1α-HCA). However, they demonstrated that MRI cannot classify HCAs when necrotic/hemorrhagic changes cover > 50% of the lesion, HNF1α-HCAs does not show steatosis and when HCA subtype is β-HCA or U-HCAs (43).

Typical imaging findings of HCA are heterogeneous signal intensity on T1- and T2-weighted images and heterogeneous iso or hypodensity on unenhanced CT due to the presence of hemorrhage, necrosis, or intralesional fat **(fig. 2)**. On contrast-enhanced imaging, HCA typically demonstrates moderate to intense enhancement in the arterial phase and prolonged mild enhancement or washing out on the portal venous phase. On hepatocyte phase images of HB contrast-enhanced MRI, HCA typically appears hypointense compared to the adjacent liver parenchyma (35, 38).

I-HCA is the most common subtype representing 30%-50% of HCAs. The hallmark feature for I-HCA is the "atoll sign" on T2-weighted images described as a band of peripheral T2 hyperintense signal. I-HCA may show imaging features that overlap with FNH. They are hypervascular masses that demonstrate intense arterial enhancement with persistent enhancement on portal venous and delayed phases. Different from other adenoma subtypes, on HB phase I-HCAs can appear iso- to hyperintense compared to the background parenchyma probably due to retention of contrast material within dilated intratumoral sinusoids. The clue to differentiate I-HCA from FNH is the signal intensity on the HB phase not as homogeneous as FNH, and often the hyperenhancement is only peripheral (42). T2 signal hyperintensity associated with strong arterial phase enhancement and delayed persistent enhancement on

MRI enable diagnosis of I-HCA with a sensitivity of 85–88% and a specificity of 88–100% (41).

HNF1α-HCA is the second most common subtype, and histologically is characterized by intracellular fat deposition. Therefore, a signal dropout on opposed-compared with in-phase T1-weighted images had a reported sensitivity of 86% and a specificity of 100% for HNF1α-HCA (42).

β-HCA is less common (approximately 10% of all HCAs) and occurs more in men. This subtype has a higher risk of malignant transformation. The imaging features of β-HCA are not specific and mimic HCCs. On contrast-enhanced MRI, β-HCAs demonstrate homogenous or heterogeneous arterial phase hyperenhancement with possible wash-out on portal venous

phase. Also, these tumors can show a capsule appearance as HCC. On diffusion-weighted imaging (DWI), the absence of restriction can be useful to distinguish benign lesions from HCC **(fig. 2),** although also HCA could sometimes show restricted diffusion (42). Besides, these tumors can show a vaguely demarcated central scar and appear iso- to hyperintense relative to the liver parenchyma on the HB phase, so that the differential diagnosis from FNH could be a challenge.

Finally, no specific imaging features have been described for unclassified HCA (41, 42).

In conclusion, in the absence of typical features of HCA on MRI, a tumor biopsy should be proposed to rule out malignancy (27).
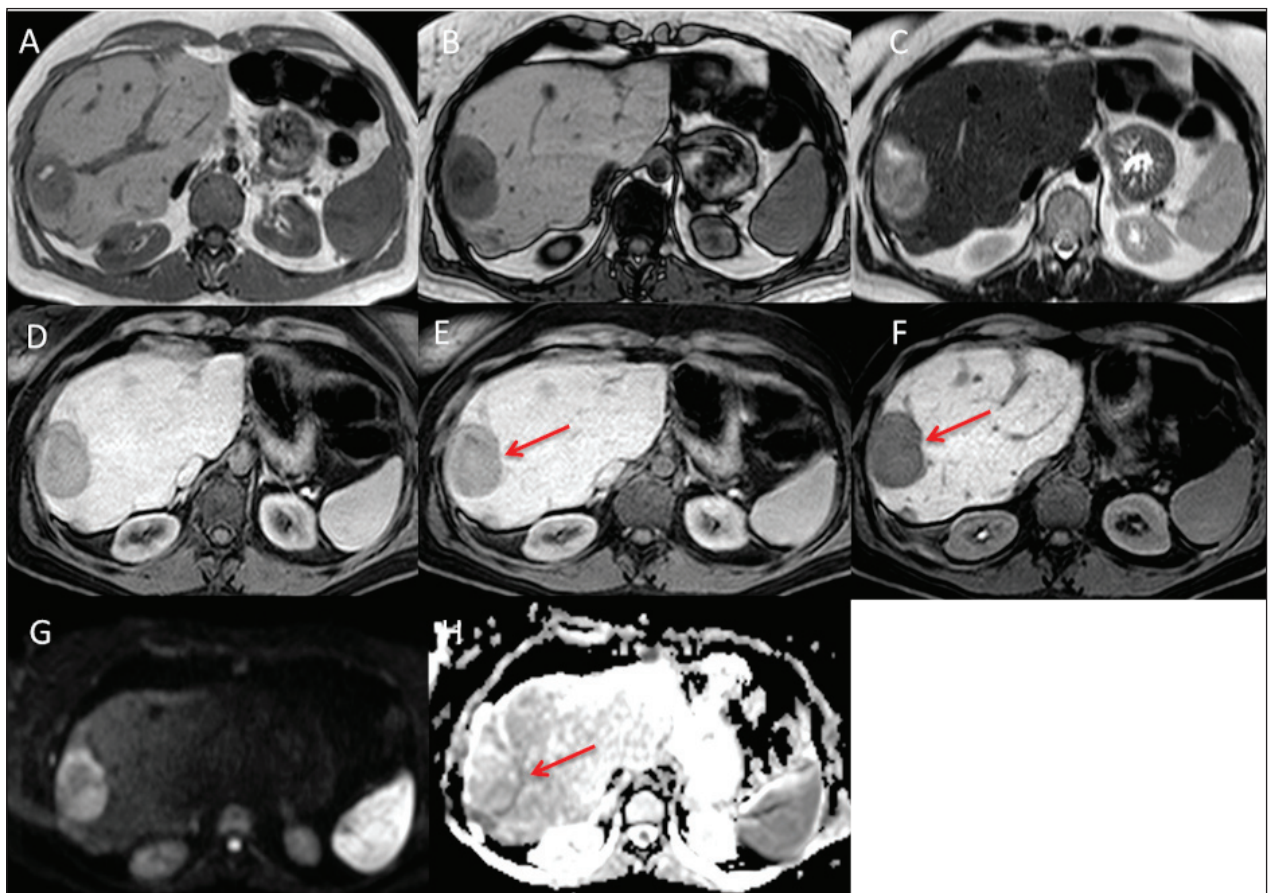

Figure 2. β-HCA on Gd-BOPTA-enhanced MRI. β-HCA shows heterogeneous signal intensity on T1- (A) and T2-weighted (C) with a signal dropout on opposed-phase T1-weighted image (B) due to the presence of hemorrhage and intralesional fat. On contrast-enhanced imaging, β-HCA demonstrates moderate enhancement in the arterial phase (D) and prolonged mild enhancement on the portal venous phase (E). On hepatocyte phase (F), β-HCA appears hypointense compared to the adjacent liver parenchyma. The presence of a capsule appearance (arrows) leads to differential diagnosis from HCC. On DWI (G-H) the absence of diffusion restriction is useful to distinguish β-HCA from HCC

Hepatocellular Carcinoma

HCC is the most common primary hepatic malignant tumor and typically develops in a cirrhotic liver (42, 44). According to international guidelines, including those of the European Association for the Study of the Liver and the American Association for the Study of Liver Disease, HCC can be diagnosed noninvasively using contrast-enhanced CT or MRI based on its typical vascular pattern (37, 45). Imaging modalities also play a fundamental role in guiding interventional radiology procedures, as well as in surgical planning and follow-up (46-57). The hallmark imaging features of HCC are arterial phase hyperenhancement (wash-in) and hypoenhancement on portal or delayed phase images (wash-out) (42, 58, 59). However, approximately 40% of HCC nodules show atypical imaging features, so that diagnosis remains a challenge for radiologists (42).

The typical enhancement pattern of HCCs is due to a multistep process of arterialization of the nodule. During the multistep process of hepatocarcinogenesis, a sequential decrease in the portal blood supply and development of neoangiogenesis with an increase in the hepatic arterial blood supply occurs (58, 60). The imaging features of HCC vary significantly with the histological classification and with the size of the lesion. Typically HCCs are hypointense on T1-weighted images and hyperintense on T2-weighted images. However, early HCCs (defined as a well-differentiated tumor <2 cm in size) can show iso- or hyperintensity on T1-weighted images because of the accumulation of fat, glycoproteins, or copper (42, 60, 61). Large HCCs may have a mosaic pattern with areas of variable signal intensities on T1- and T2-weighted images and heterogeneous enhancement on contrast-

enhanced images during the arterial phase (60). Poorly differentiated and undifferentiated HCCs may show a tumor capsule that appears hypointense on both T1- and T2-weighted images. The tumor capsule appears as a peripheral rim enhancement on the portal venous phase that has to be differentiated from arterial rim enhancement, which is common in intrahepatic cholangiocarcinoma (ICC) or metastases from adenocarcinoma (42, 60, 62).

Early HCCs are hypovascular nodule due to decreased portal venous blood supply and insufficient neovascularization. As a result, 10-20% of HCCs do not show typical arterial phase wash-in and are detected only in the portal venous or delayed phase as hypoenhancing nodules **(fig. 3)**. The differential diagnosis of hypovascular HCC from DN is a challenge, but several studies have reported that features as hypointensity on T1-weighted imaging, hyperintensity on T2-weighted imaging, and diffusion restriction on DWI help in distinguishing early HCCs from DNs (42, 58, 63). Several studies have demonstrated that HB contrast agents represent useful tools for the detection and characterization of atypical HCC nodules, such as hypovascular HCC (64). HB contrast agents are transported into the hepatocytes through the molecular transporter organic anion-transporting polypeptide 8 (OATP8) that are downregulated in HCC nodules. Therefore, hypointensity on the HB phase is strongly suggestive of almost all HCCs and some high-grade DNs (58, 64). Recent studies reported that the decreased expression of OATP8 precedes the neoangiogenesis among these nodules demonstrating that hepatobiliary phase imaging improves the diagnosis of HCCs (58). Galia M. et al. analyzed 69 indeterminate hepatocellular nodules demonstrating that hepatobiliary phase hypointensity is weakly associated with
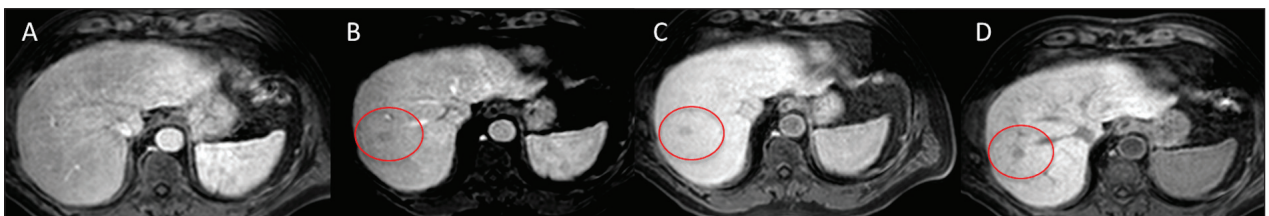

Figure 3. Atypical HCC on Gd-BOPTA-enhanced MRI. Hypovascular HCC does not show typical arterial phase wash-in (A), but it is detected in the portal venous (B) and delayed phase (C) as a hypoenhancing nodule (circle). On the hepatobiliary phase, hypovascular HCC appears hypointense (D)

HCC development (65). In this setting, the Asian Pacific Association for the Study of the Liver and the Korean Liver Cancer Study Group and the National Cancer Center guidelines suggest hypointensity on hepatobiliary phase as an alternative sign to wash-out on the portal venous phase (42). Nevertheless, a minority of HCCs (approximately 5–12%) appears iso or hyperintense relative to background parenchyma in the hepatocyte phase for increased expression of OATP8 in well- or moderately-differentiated lesions (35, 37, 66). Iannicelli E. et al., in their study on 120 suspected hepatic nodules in patients with chronic liver disease, reported two lesions appearing hyperintense in the hepatobiliary phase images; these nodules were well-differentiated HCCs at histological examination (58). Radiologists need to be familiar with this diagnostic pitfall to differentiate atypical HCCs from FNHs (67). The clues to the correct diagnosis of HCCs may be ancillary features such as a hypointense rim on the HB phase and absence of a central scar **(fig. 4)** (42).

When MRI is performed with gadoxetate disodium (Eovist Bayer HealthCare; Primovist, Bayer Schering Pharma) as HB contrast agent, the radiologist must pay attention to the "pseudo-washout" phenomenon (68). When this HB contrast agent is used,

hemangiomas appear hypointense compared to the surrounding parenchyma in the equilibrium phase due to rapid contrast uptake by the adjacent normal parenchyma. This is known as the "pseudo-washout" phenomenon and lead to differentiate especially high-flow hemangioma from hypervascular hepatic tumors, such as HCC (68, 69). The keys to differentiate hemangiomas from malignant lesions are very high signal on T2- and heavily T2-weighted images and no restriction on DWI. Finally, the diagnosis can be confirmed with CT or with MRI performed with an extracellular contrast agent (35, 63, 68).

Small HCCs often do not show portal or delayed phase wash-out at dynamic CT or MR images appearing isointense. This atypical enhancement pattern causes difficult differential diagnoses with non-neoplastic arterial-enhancing pseudolesions commonly found in cirrhotic liver, such as arterioportal shunts. DWI and MR hepatobiliary contrast agents may be helpful because arterioportal shunts usually show no diffusion restriction and are isointense on hepatobiliary phase, instead of HCC. The nodule-in-nodule is another atypical radiologic feature of HCC. It is defined as a tumor focus within a high-grade dysplastic nodule. On enhanced CT o MR images, the central HCC focus appears as
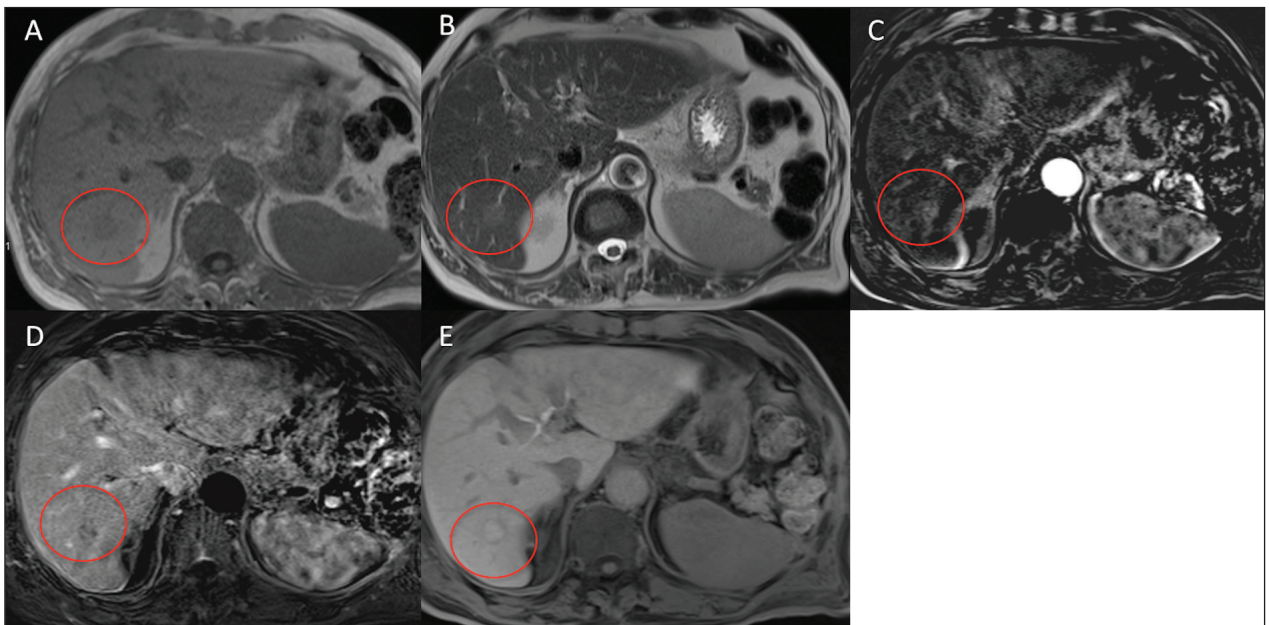

Figure 4. Well-differentiated HCC on Gd-BOPTA-enhanced MRI. HCC (circle) shows a slight hypointensity on T1-weighted image (A), slight hyperintensity on T2-weighted image (B), and typical arterial wash-in (C) and wash-out on portal phase (D). HCC appears hyperintense relative to background parenchyma in the hepatocyte phase (E) with a hypointense peripheral rim

a focus of arterial phase hyperenhancement inside a less enhancing nodule. On T1-weighted images, the background nodule often has a higher signal intensity, while on T2-weighted images the inner focus of HCC is hyperintense. The inner HCC focus shows diffusion restriction on DWI (42, 63).

Approximately 7-13% of HCCs do not appear as a nodule but as a mass with ill-defined and invasive borders, and they are called infiltrative HCCs. Portal vein tumor thrombosis is often a primary imaging feature of these atypical HCCs and can affect the hemodynamics of the tumor so that infiltrative HCCs may not exhibit the hallmark imaging features of wash in and wash-out. In this setting, the correct diagnosis is difficult, and the differential diagnosis should include ICC. Multidisciplinary discussion and laboratory data, such as elevated alpha-fetoprotein levels, may help diagnose infiltrative HCCs correctly (42).

Among the HCC variants, those with targetoid appearance include scirrhous HCCs and large HCCs (≥5 cm) with central necrosis/ischemia. The enhancement pattern of scirrhous HCCs is determined by central fibrosis within the tumor. On dynamic CT and MRI, scirrhous HCCs show peripheral rim enhancement on the arterial phase with a delayed enhancement of the central region. Also, scirrhous HCCs often showed the targetoid appearance on the HB phase, defined as peripheral hypointensity. Therefore, it is critical to differentiate scirrhous HCCs from ICCs characterized by the targetoid appearance on dynamic or HB imaging as well as on DWI. Ancillary features such as heterogeneous hyperintensity with central dark area on T2-weighted images or a capsule are more favorable for scirrhous HCCs in comparison with ICCs. On the contrary, the absence of the wash-out appearance, surface retraction, and presence of bile duct dilatation is helpful features in distinguishing ICCs from scirrhous HCCs. According to the Liver Imaging Reporting and Data System (LI-RADS), hepatic tumors with arterial rim enhancement should be categorized as probably or definitely malignant but not HCC specific, and liver biopsy is warranted for a confirmative diagnosis (42).

In conclusion, a definitive diagnosis of HCC cannot be made with dynamic CT or MRI without the hallmark features. Therefore the majority of interna-

tional guidelines recommend liver biopsy in atypical HCC nodules larger than 1cm (65).

Conflict of interest: Authors declare that they have no commercial associations (e.g. consultancies, stock ownership, equity interest, patent/licensing arrangement etc.) that might pose a conflict of interest in connection with the submitted article.

References

1. Lo RC, Ng IO. Hepatocellular tumors: immunohistochemical analyses for classification and prognostication. Chin J Cancer Res 2011; 23: 245-53.
2. Mazzei MA, Squitieri NC, Sani E, et al. Differences in perfusion CT parameter values with commercial software upgrades: a preliminary report about algorithm consistency and stability. Acta Radiol 2013; 54: 805-11.
3. Hori M, Murakami T, Kim T, Tomoda K, Nakamura H. CT Scan and MRI in the Differentiation of Liver Tumors. Dig Dis. 2004;22:39-55.
4. Nowicki TK, Markiet K, Izycka-Swieszewska E, Dziadziuszko K, Studniarek M, Szurowska E. Efficacy comparison of multi-phase CT and hepatotropic contrast-enhanced MRI in the differential diagnosis of focal nodular hyperplasia: a prospective cohort study. BMC Gastroenterol. 2018;18:10.
5. Pesapane F, Patella F, Fumarola EM, et al. Intravoxel Incoherent Motion (IVIM) Diffusion Weighted Imaging (DWI) in the Periferic Prostate Cancer Detection and Stratification. Med Oncol 2017; 34: 35.
6. Zhang YD, Zhu FP, Xu X, et al. Liver Imaging Reporting and Data System:Substantial Discordance Between CT and MR for Imaging Classification of Hepatic Nodules. Acad Radiol. 2016;23:344-352.
7. Marampon F, Gravina GL, Popov VM, et al. Close correlation between MEK/ERK and Aurora-B signaling pathways in sustaining tumorigenic potential and radioresistance of gynecological cancer cell lines. Int J Oncol 2014; 44: 285-94.
8. Chou R, Cuevas C, Fu R, et al. Imaging Techniques for the Diagnosis of Hepatocellular Carcinoma: A Systematic Review and Meta-analysis. Ann Intern Med. 2015;162:697-711.
9. Kurucay M, Kloth C, Kaufmann S, et al. Multiparametric imaging for detection and characterization of hepatocellular carcinoma using gadoxetic acid-enhanced MRI and perfusion-CT: which parameters work best?. Cancer Imaging. 2017;17:18.
10. Agliata G, Schicchi N, Agostini A, et al. Radiation exposure related to cardiovascular CT examination: comparison between conventional 64-MDCT and third-generation dual-source MDCT. Radiol Med 2019; 124: 753-61.
11. Lamba R, Fananapazir G, Corwin MT, Khatri VP. Diagnostic imaging of hepatic lesions in adults. Surg Oncol Clin N Am. 2014;23:789-820

12. Reginelli A, Silvestro G, Fontanella G, et al. Performance status versus anatomical recovery in metastatic disease: The role of palliative radiation treatment. Int J Surg 2016; 33 Suppl 1: S126-31.

13. Barabino M, Gurgitano M, Fochesato C, et al. LI-RADS to categorize liver nodules in patients at risk of HCC: tool or a gadget in daily practice?. Radiol Med. 2020;10.1007s11547-020-01225-8.

14. Baker FA, Zeina AR, Mouch SA, Mari A. Benign Hepatic Tumors: From Incidental Imaging Finding to Clinical Management. Korean J Fam Med. 2020;10.4082/kjfm.18.0188.

15. Alenezi AO, Krishna S, Mendiratta-Lala M, Kielar AZ. Imaging and Management of Liver Cancer. Semin Ultrasound CT MR. 2020;41:122-138.

16. Hartke J, Johnson M, Ghabril M. The diagnosis and treatment of hepatocellular carcinoma. Semin Diagn Pathol.2017;34:153-159.

17. Wu M, Li L, Wang J, et al. Contrast-enhanced US for characterization of focal liver lesions: a comprehensive meta-analysis. Eur Radiol. 2018;28:2077-2088.

18. Battaglia V, Cervelli R. Liver investigations: Updating on US technique and contrast-enhanced ultrasound (CEUS). Eur J Radiol. 2017;96:65-73

19. Donato H, França M, Candelária I, Caseiro-Alves F. Liver MRI: From basic protocol to advanced techniques. Eur J Radiol. 2017;93:30-39.

20. Haimerl M, Wächtler M, Platzek I, et al. Added value of Gd-EOB-DTPA-enhanced Hepatobiliary phase MR imaging in evaluation of focal solid hepatic lesions. BMC Med Imaging. 2013;13:41.

21. Agostini A, Mari A, Lanza C, et al. Trends in radiation dose and image quality for pediatric patients with a multidetector CT and a third-generation dual-source dual-energy CT. Radiol Med 2019; 124: 745-52.

22. Curtis WA, Fraum TJ, An H, Chen Y, Shetty AS, Fowler KJ. Quantitative MRI of Diffuse Liver Disease: Current Applications and Future Directions. 2019, Radiology. 290(1):23-30

23. Elsayes KM, Menias CO, Morshid AI, et al. Spectrum of Pitfalls, Pseudolesions, and Misdiagnoses in Noncirrhotic Liver. AJR Am J Roentgenol 2018; 211: 97-108.

24. Ito K, Honjo K, Fujita T, et al. Liver neoplasms: diagnostic pitfalls in cross-sectional imaging. Radiographics 1996; 16: 273-93.

25. Hoodeshenas S, Yin M, Venkatesh SK. Magnetic Resonance Elastography of Liver: Current Update. Top Magn Reson Imaging. 2018 27(5):319-333

26. Asbach P, Klessen C, Koch M, Hamm B, Taupitz M. Magnetic resonance imaging findings of atypical focal nodular hyperplasia of the liver. Clin Imaging 2007; 31: 244-52.

27. Roncalli M, Sciarra A, Tommaso LD. Benign hepatocellular nodules of healthy liver: focal nodular hyperplasia and hepatocellular adenoma. Clin Mol Hepatol 2016; 22: 199-211.

28. Husainy MA, Sayyed F, Peddu P. Typical and atypical benign liver lesions: A review. Clin Imaging 2017; 44: 79-91.

29. Cellina M, Oliva G, Menozzi A, Soresina M, Martinenghi C, Gibelli D. Non-contrast Magnetic Resonance Lymphangiography: an emerging technique for the study of lymphedema. Clin Imaging 2019; 53: 126-33.

30. Alobaidi M, Shirkhoda A. Benign focal liver lesions: discrimination from malignant mimickers. Curr Probl Diagn Radiol 2004; 33: 239-53.

31. Marin D, Brancatelli G, Federle MP, et al. Focal nodular hyperplasia: typical and atypical MRI findings with emphasis on the use of contrast media. Clin Radiol 2008; 63: 577-85.

32. Vernuccio F, Ronot M, Dioguardi Burgio M, et al. Uncommon evolutions and complications of common benign liver lesions. Abdom Radiol (NY) 2018; 43: 2075-96.

33. Scialpi M, Palumbo B, Pierotti L, et al. Detection and characterization of focal liver lesions by split-bolus multidetector-row CT: diagnostic accuracy and radiation dose in oncologic patients. Anticancer Res 2014; 34: 4335-44.

34. Grazioli L, Morana G, Kirchin MA, Schneider G. Accurate differentiation of focal nodular hyperplasia from hepatic adenoma at gadobenate dimeglumine-enhanced MR imaging: prospective study. Radiology 2005; 236: 166-77.

35. Scali EP, Walshe T, Tiwari HA, Harris AC, Chang SD. A Pictorial Review of Hepatobiliary Magnetic Resonance Imaging With Hepatocyte-Specific Contrast Agents: Uses, Findings, and Pitfalls of Gadoxetate Disodium and Gadobenate Dimeglumine. Can Assoc Radiol J 2017; 68: 293-307.

36. Furlan A, Brancatelli G, Dioguardi Burgio M, et al. Focal Nodular Hyperplasia After Treatment With Oxaliplatin: A Multiinstitutional Series of Cases Diagnosed at MRI. AJR Am J Roentgenol 2018; 210: 775-79.

37. Agostini A, Kircher MF, Do RK, et al. Magnetic Resonanance Imaging of the Liver (Including Biliary Contrast Agents)-Part 2: Protocols for Liver Magnetic Resonanance Imaging and Characterization of Common Focal Liver Lesions. Semin Roentgenol 2016; 51: 317-33.

38. Murakami T, Tsurusaki M. Hypervascular benign and malignant liver tumors that require differentiation from hepatocellular carcinoma: key points of imaging diagnosis. Liver Cancer 2014; 3: 85-96.

39. Kim MJ, Lee S, An C. Problematic lesions in cirrhotic liver mimicking hepatocellular carcinoma. Eur Radiol 2019; 29: 5101-10.

40. Carrafiello G, Fontana F, Cotta E, et al. Ultrasound-guided thermal radiofrequency ablation (RFA) as an adjunct to systemic chemotherapy for breast cancer liver metastases. Radiol Med 2011; 116: 1059-66.

41. Zulfiqar M, Sirlin CB, Yoneda N, et al. Hepatocellular adenomas: Understanding the pathomolecular lexicon, MRI features, terminology, and pitfalls to inform a standardized approach. J Magn Reson Imaging 2019;

42. Kim JH, Joo I, Lee JM. Atypical Appearance of Hepatocellular Carcinoma and Its Mimickers: How to Solve Challenging Cases Using Gadoxetic Acid-Enhanced Liver Magnetic Resonance Imaging. Korean J Radiol 2019; 20: 1019-41.

43. Bise S, Frulio N, Hocquelet A, et al. New MRI features improve subtype classification of hepatocellular adenoma. Eur Radiol 2019; 29: 2436-47.

44. Petrillo M, Patella F, Pesapane F, et al. Hypoxia and tumor angiogenesis in the era of hepatocellular carcinoma transarterial loco-regional treatments. Future Oncol 2018; 14: 2957-67.

45. Agostini A, Kircher MF, Do R, et al. Magnetic Resonance Imaging of the Liver (Including Biliary Contrast Agents) Part 1: Technical Considerations and Contrast Materials. Semin Roentgenol 2016; 51: 308-16.

46. Nicolini D, Agostini A, Montalti R, et al. Radiological response and inflammation scores predict tumour recurrence in patients treated with transarterial chemoembolization before liver transplantation. World J Gastroenterol 2017; 23: 3690-701.

47. Floridi C, Radaelli A, Pesapane F, et al. Clinical impact of cone beam computed tomography on iterative treatment planning during ultrasound-guided percutaneous ablation of liver malignancies. Med Oncol 2017; 34: 113.

48. Panfili E, Nicolini D, Polverini V, Agostini A, Vivarelli M, Giovagnoni A. Importance of radiological detection of early pulmonary acute complications of liver transplantation: analysis of 259 cases. Radiol Med 2015; 120: 413-20.

49. Greco F, Autorino R, Altieri V, et al. Ischemia Techniques in Nephron-sparing Surgery: A Systematic Review and Meta-Analysis of Surgical, Oncological, and Functional Outcomes. Eur Urol 2019; 75: 477-91.

50. Ingraham C, Johnson G, Padia SA, Vaidya S. Interventional Radiology for Liver Lesions. Semin Roentgenol. 2016;51:367-377.

51. Cornelis FH, Borgheresi A, Petre EN, Santos E, Solomon SB, Brown K. Hepatic Arterial Embolization Using Cone Beam CT with Tumor Feeding Vessel Detection Software: Impact on Hepatocellular Carcinoma Response. Cardiovasc Intervent Radiol 2018; 41: 104-11.

52. Gonzalez-Guindalini FD, Botelho MP, Harmath CB, et al. Assessment of liver tumor response to therapy: role of quantitative imaging. Radiographics. 2013;33:1781-1800.

53. Carrafiello G, D'Ambrosio A, Mangini M, et al. Percutaneous cholecystostomy as the sole treatment in critically ill and elderly patients. Radiol Med 2012; 117: 772-9.

54. Carrafiello G, Ierardi AM, Piacentino F, Cardim LN. Percutaneous transhepatic embolization of biliary leakage with N-butyl cyanoacrylate. Indian J Radiol Imaging 2012; 22: 19-22.

55. Lucchina N, Tsetis D, Ierardi AM, et al. Current role of microwave ablation in the treatment of small hepatocellular carcinomas. Ann Gastroenterol 2016; 29: 460-65.

56. Ippolito D, Inchingolo R, Grazioli L, et al. Recent advances in non-invasive magnetic resonance imaging assessment of hepatocellular carcinoma. World J Gastroenterol. 2018;24:2413-2426.

57. Belfiore MP, Reginelli A, Maggialetti N, et al. Preliminary results in unresectable cholangiocarcinoma treated by CT percutaneous irreversible electroporation: feasibility, safety and efficacy. Med Oncol 2020; 37: 45.

58. Iannicelli E, Di Pietropaolo M, Marignani M, et al. Gadoxetic acid-enhanced MRI for hepatocellular carcinoma and hypointense nodule observed in the hepatobiliary phase. Radiol Med 2014; 119: 367-76.

59. Borgheresi A, Gonzalez-Aguirre A, Brown KT, et al. Does Enhancement or Perfusion on Preprocedure CT Predict Outcomes After Embolization of Hepatocellular Carcinoma? Acad Radiol 2018; 25: 1588-94.

60. Jeong YY, Yim NY, Kang HK. Hepatocellular carcinoma in the cirrhotic liver with helical CT and MRI: imaging spectrum and pitfalls of cirrhosis-related nodules. AJR Am J Roentgenol 2005; 185: 1024-32.

61. Venturini M, Angeli E, Maffi P, et al. Liver focal fatty changes at ultrasound after islet transplantation: an early sign of altered graft function? Diabet Med 2010; 27: 960-4.

62. Vernuccio F, Cannella R, Porrello G, et al. Uncommon imaging evolutions of focal liver lesions in cirrhosis. Abdom Radiol (NY) 2019; 44: 3069-77.

63. Elsayes KM, Chernyak V, Morshid AI, et al. Spectrum of Pitfalls, Pseudolesions, and Potential Misdiagnoses in Cirrhosis. AJR Am J Roentgenol 2018; 211: 87-96.

64. Bargellini I, Battaglia V, Bozzi E, Lauretti DL, Lorenzoni G, Bartolozzi C. Radiological diagnosis of hepatocellular carcinoma. J Hepatocell Carcinoma 2014; 1: 137-48.

65. Galia M, Agnello F, Sparacia G, et al. Evolution of indeterminate hepatocellular nodules at Gd-EOB-DPTA-enhanced MRI in cirrhotic patients. Radiol Med 2018; 123: 489-97.

66. Park HJ, Choi BI, Lee ES, Park SB, Lee JB. How to Differentiate Borderline Hepatic Nodules in Hepatocarcinogenesis: Emphasis on Imaging Diagnosis. Liver Cancer 2017; 6: 189-203.

67. Pinto A, Caranci F, Romano L, Carrafiello G, Fonio P, Brunese L. Learning from errors in radiology: a comprehensive review. Semin Ultrasound CT MR 2012; 33: 379-82.

68. Doo KW, Lee CH, Choi JW, Lee J, Kim KA, Park CM. "Pseudo wash-out" sign in high-flow hepatic hemangioma on gadoxetic acid contrast-enhanced MRI mimicking hypervascular tumor. AJR Am J Roentgenol 2009; 193: W490-6.

69. Pradella S, Lucarini S, Colagrande S. Liver lesion characterization: the wrong choice of contrast agent can mislead the diagnosis of hemangioma. AJR Am J Roentgenol 2012; 199: W662.

Correspondence:
Giulia Grazzini
Department of Radiology, Careggi University Hospital
L.go Brambilla, 3
50134 – Florence – Italy
E-mail: grazzini.giulia@gmail.com